

ACTIVE AND PASSIVE RADIATIVE TRANSFER SIMULATIONS FOR GPM-RELATED FIELD CAMPAIGNS

*Ian S. Adams, S. Joseph Munchak, Kwo-Sen Kuo, Craig Pelissier,
Thomas Clune, Rachael Kroodsma, Adrian Loftus, and Xioawen Li**

NASA Goddard Space Flight Center
Greenbelt, MD 20771

ABSTRACT

Using a three-dimensional radiative transfer model combined with cloud-resolving model output, we simulate active and passive sensor observations of clouds and precipitation. This combination of tools allows us to diagnose the contributions of various hydrometeor types. Radar multiple scattering is most closely associated with the presence of graupel. At W-band, massive amounts multiple scattering in deep convection can decorrelate the reflectivity profile from the vertical structure, but for less intense events, multiple scattering could be a useful indicator of riming. For passive sensors, polarization differences at 166 GHz indicate the presence of horizontally-aligned frozen particles with pronounced aspect ratios, while high concentrations of more isotropic aggregates and graupel dampen the polarization difference while also contributing to the lowest brightness temperature depressions. The insights into remote sensing measurements will facilitate the development of improved algorithms and advanced sensors.

Index Terms— Radar, radiometer, clouds, precipitation, radiative transfer

1. INTRODUCTION

Frozen precipitation is a key component of the global water cycle. It provides rainfall through cold rain processes and snowfall which is a primary source of drinking and irrigation water, particularly near mountainous regions. Given the importance of precipitation to societal applications, understanding how different species of hydrometeors affect remote sensing observations will allow researchers to develop advanced algorithms that can better utilize available data and to plan more effective architectures for future missions, such as for the Clouds, Convection, and Precipitation observable designated by the 2018 Earth Science Decadal Survey.

*Drs. Kuo, Kroodsma, and Loftus are also with the University of Maryland, Dr. Pelissier is also with SSAI, and Dr. Li is also with Morgan State University

2. SIMULATION DESCRIPTION

To perform radiative transfer simulations, we used the Atmospheric Radiative Transfer Simulator (ARTS), version 2.3 [1]. For passive simulations, we used reverse Monte Carlo integration [2] to fully account for three-dimensional spatial effects within a dichroic, or polarizing, medium. Radar multiple scattering calculations employed forward Monte Carlo integration. Hydrometeor scattering properties for rain and cloud liquid were calculated using the T-Matrix method [3], and the complex permittivity was calculated using a parameterization specifically targeted to supercooled liquid water in the microwave regime [4]. Randomly oriented snow and graupel scattering properties were taken from the ARTS database [5], while horizontally aligned ice particles, assuming plate-like geometries, were calculated using the Invariant Imbedding T-Matrix Method (IITM) which allows for significantly higher aspect ratios than traditional T-Matrix codes. A temperature-dependent complex permittivity fit was used for ice [6]. Gas absorption lookup tables were computed using the Rosenkranz absorption model [7, 8, 9, 10]. Since the scenarios used in this study occur over land, a blackbody background is used for the passive simulations. The surface is not considered for the radar simulations. Brightness temperature results are given in terms of the first two Stokes elements using the following convention:

$$I = \frac{1}{2} (Tb_v + Tb_h) \quad (1)$$

$$Q = \frac{1}{2} (Tb_v - Tb_h). \quad (2)$$

As input to the radiative transfer model, we used cloud resolving simulation data from the NASA Unified Weather Research and Forecasting (NU-WRRF) model. Such datasets are ideal for populating ARTS, providing three-dimensional fields of temperature, pressure/height, water vapor, as well as a number of hydrometeor species: rain, cloud liquid, cloud ice, graupel, and snow. The simulations correspond to ground validation campaigns related to NASA's Global Precipitation Measurement (GPM) mission: the Mid-latitude Continental Convective Clouds Experiment (MC3E) and the

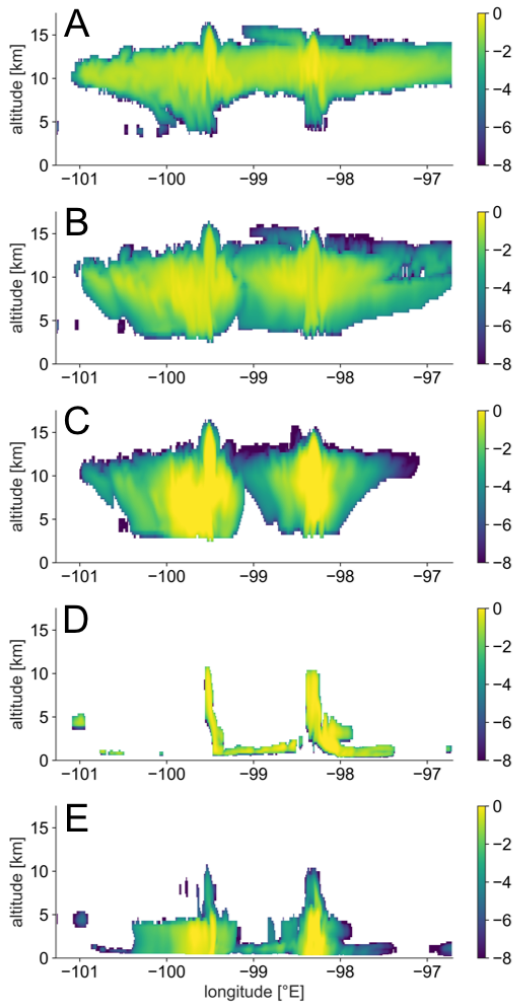


Fig. 1. Two-dimensional curtain of mixing Ratios of (A) cloud ice, (B) snow, (C) graupel, (D) cloud liquid, and (E) rain from 20 May 2011 MC3E simulation, 0600 UTC timestep.

Olympic Mountains Experiment (OLYMPEX). Morrison double-moment microphysics [11] were used for all hydrometeor species, with the exception of single moment for cloud liquid in the MC3E simulation.

3. RESULTS

Figure 1 shows a curtain of cloud and precipitation mixing ratios from the 0600 UTC timestep for the 20 May 2011 MC3E simulation. The anvil is composed primarily of cloud ice, while the cores are a mix of snow and graupel. W-band radar reflectivities exhibit significant attenuation and multiple scattering where graupel is present (Fig. 2), but the multiple scattering effects are localized at the bottom of the convective towers for Ka-band (not shown). Given the magnitude of the multiple scattering signatures, and the attenuation of

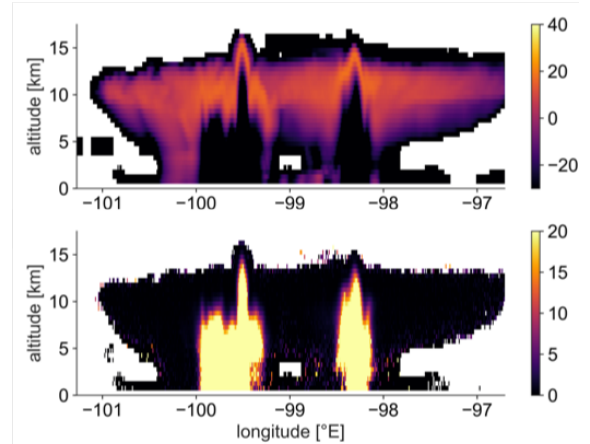


Fig. 2. Curtains of radar reflectivity (top) and multiple scattering enhancement (bottom) at W-band corresponding to Fig. 1.

the backscatter profile from the clouds and precipitation, retrievals of microphysical parameters using W-band radar is not possible in these conditions.

Passive millimeter wave simulations at 166 GHz, at approximately 53° incidence, similar to the the GPM Microwave Imager (GMI) 165-GHz channel, show large polarization differences due to the presence of horizontally-aligned cloud ice particles (Fig. 3). When compared with airborne measurements from the Conically-Scanning Microwave Imaging Radiometer (CoSMIR) or GMI, the simulations match the overall behavior of first increasing, then decreasing, polarization difference with deepening brightness temperature depression, but the magnitude of the simulations is about a factor of two larger than observations.

The cloud and precipitation mixing ratio curtains for the OLYMPEX case are shown in Fig. 4, showing a post-frontal system approaching the windward side of the mountains. While also a convective system, the precipitation is much less intense and shallower than the MC3E case. Multiple scattering is much less of a factor at W-band (Fig. 5) and is negligible at lower frequencies.

Simulations of polarization difference, Fig. 6 show a similar increase Q with deepening brightness temperature depressions; however, Q does not turn over as the OLYMPEX simulations do not include the deep convection seen during MC3E. Also, unlike the MC3E simulations, polarization difference is not overestimated when compared with observations.

4. CONCLUSIONS

Three-dimensional radiative transfer simulations for both radars and radiometers using cloud resolving models allow us to investigate the effects of different frozen hydrometeor species. Graupel is associated with multiple scattering, and

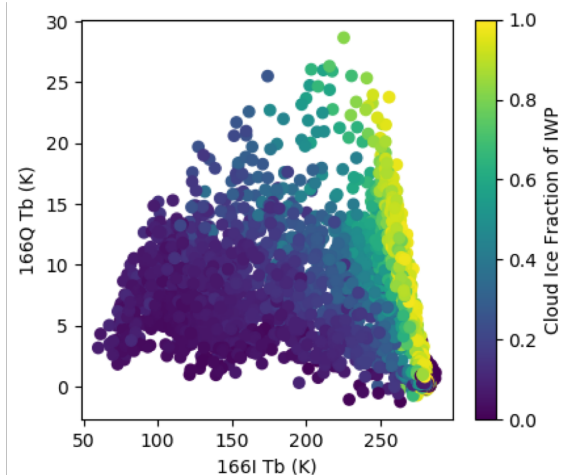


Fig. 3. Polarization difference simulations for the MC3E case, 2300 UTC timestep, plotted as Q versus I, with colorbar showing the fraction of cloud ice with respect to total ice.

the effect increases with frequency. In deep convection, large multiple scattering contributions can contaminate W-band reflectivities such that meaningful retrievals are not possible. In more moderate precipitation, multiple scattering may be an indicator of heavy riming, and thus may be useful information. Passive microwave polarization differences are an indicator of the presence of aligned hydrometeors, and may be used to differentiate convective cores from anvil regions. Future work should include a wider range of ice particles, including aligned aggregates and other cloud ice particles. For example, columns and rosettes would be more appropriate for convective simulations. This may be one source of the large mismatch in polarization difference between simulations and observations for the MC3E case, but other factors may contribute, including the representativeness of the cloud simulations.

5. REFERENCES

- [1] S. A. Buehler, J. Mendrok, P. Eriksson, A. Perrin, R. Larsson, and O. Lemke, “ARTS, the atmospheric radiative transfer simulator – version 2.2, the planetary toolbox edition,” *Geosci. Model Dev.*, vol. 11, no. 4, pp. 1537–1556, 2018.
- [2] C. Davis, C. Emde, and R. Harwood, “A 3D polarized reverse Monte Carlo radiative transfer model for mm and sub-mm passive remote sensing in cloudy atmospheres,” *IEEE Trans. Geosci. Remote Sens.*, vol. 43, pp. 1096–1101, May 2005.
- [3] Michael I Mishchenko and Larry D Travis, “Capabilities and limitations of a current FORTRAN implementation of the T-matrix method for randomly oriented, rotation-ally symmetric scatterers,” *J. Quant. Spectrosc. Rad. Trans.*, vol. 60, pp. 309–324, Sep 1998.
- [4] D.D. Turner, S. Kneifel, and M. P. Cadetdu, “An improved liquid water absorption model at microwave frequencies for supercooled liquid water clouds,” *J. Atmos. Oceanic Technol.*, vol. 33, pp. 33–44, Jan 2016.
- [5] P. Eriksson, R. Ekelund, J. Mendrok, M. Brath, O. Lemke, and S. A. Buehler, “A general database of hydrometeor single scattering properties at microwave and sub-millimetre wavelengths,” *Earth System Science Data*, vol. 10, no. 3, pp. 1301–1326, 2018.
- [6] C. Mätzler, “Dielectric properties of natural media: microwave dielectric properties of ice,” in *Thermal Microwave Radiation: Applications for Remote Sensing*,

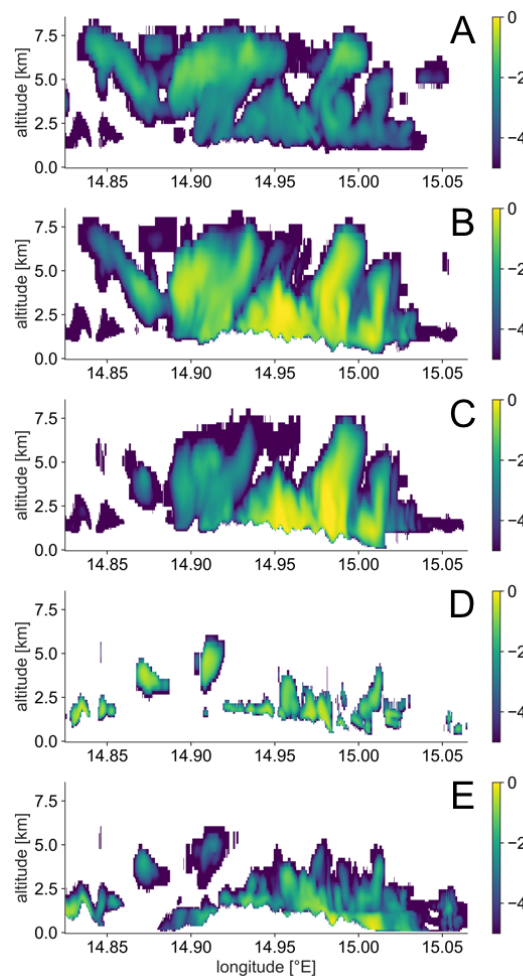


Fig. 4. Two-dimensional curtain of mixing Ratios of (A) cloud ice, (B) snow, (C) graupel, (D) cloud liquid, and (E) rain from 04 December 2015 OLYMPEX simulation, 1500 UTC timestep.

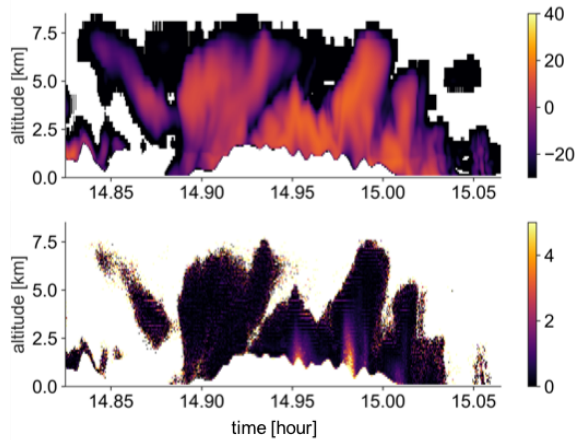


Fig. 5. Curtains of radar reflectivity (top) and multiple scattering enhancement (bottom) at W-band corresponding to Fig. 4.

C. Mätzler, Ed., pp. 455–463. The Institution of Engineering and Technology, 2006.

- [7] P. W. Rosenkranz, “Absorption of microwaves by atmospheric gasses,” in *Atmospheric Remote Sensing by Microwave Radiometry*, M A Janssen, Ed., pp. 37–90. Wiley, 1993.
- [8] P W Rosenkranz, “Water vapor microwave continuum absorption: A comparison of measurements and models,” *Radio Sci.*, vol. 33, pp. 919–928, Apr 1998.
- [9] P W Rosenkranz, “Correction to ‘water vapor microwave continuum absorption: A comparison of measurements and models’,” *Radio Sci.*, vol. 34, pp. 1025, Apr 1999.
- [10] M. Yu. Tretyakov, M.A. Koshelev, V.V. Dorovskikh, D.S. Makarov, and P.W. Rosenkranz, “60-ghz oxygen band: precise broadening and central frequencies of fine-structure lines, absolute absorption profile at atmospheric pressure, and revision of mixing coefficients,” *J. Molec. Spectrosc.*, vol. 231, pp. 1–14, May 2005.
- [11] H. Morrison, J. A. Curry, and V. I. Khvorostyanov, “A new double-moment microphysics parameterization for application in cloud and climate models. part i: Description,” *Journal of the Atmospheric Sciences*, vol. 62, no. 6, pp. 1665–1677, 2005.

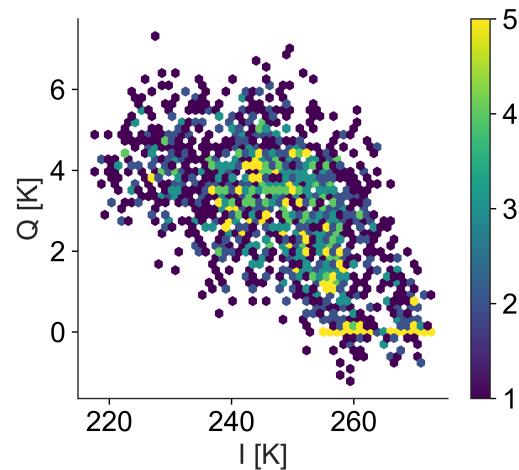


Fig. 6. Polarization difference simulations for the OLYMPEX case, plotted as Q versus I, with colorbar showing the number of points.